

## Optical and Morphological Studies on Novel Polyaniline-P<sub>2</sub>O<sub>5</sub> Conductive Polymer Composites†

P. SATHEESHKUMAR<sup>1</sup>, A. KALAIVANI<sup>2</sup>, G. SENGUTTUVAN<sup>1,\*</sup>, V. SIVAKUMAR<sup>1</sup> and C. SURENDRA DILIP<sup>3</sup>

<sup>1</sup>Department of Physics, Bharathidasan Institute of Technology, Anna University, Tiruchirappalli-620 024, India

<sup>2</sup>Department of Physics, Dhanalakshmi Srinivasan Engineering College, Perambalur 621 212, India

<sup>3</sup>Department of Chemistry, Bharathidasan Institute of Technology, Anna University, Tiruchirappalli-620 024, India

\*Corresponding author: E-mail: sengutuvan@yahoo.com

AJC-12909

Recently conducting polymer composites have attracted considerable interest due to their numerous applications. Present work reports the preparation of polyaniline polymeric material with P<sub>2</sub>O<sub>5</sub> to form polyaniline-P<sub>2</sub>O<sub>5</sub> composites by chemical oxidation method. FTIR analysis established the various modes of vibration due to diverse functional groups present in the composite and the presence of a strong interaction between P<sub>2</sub>O<sub>5</sub> and polyaniline. The UV-VIS spectra confirmed the  $\pi$ - $\pi^*$  and n- $\pi^*$  transitions of the benzenoid and quinonoid structure of the composites. The linear optical nature was understood from the optical transmission spectrum. The XRD patterns exhibited a weak crystalline nature for the composites. Thermal stability of polyaniline-P<sub>2</sub>O<sub>5</sub> was determined using TGA. The SEM images show the effect of P<sub>2</sub>O<sub>5</sub> doping and on polyaniline morphology. EDAX was performed to confirm the presence of P<sub>2</sub>O<sub>5</sub> and polyaniline. Surface topography of polyaniline-P<sub>2</sub>O<sub>5</sub> composites were studied using AFM.

**Key Words:** Polymer composites, Polyaniline, Phosphorous pentaoxide, Thermal stability, SEM, Morphology.

### INTRODUCTION

Conducting polymers with their distinctive electrical and optical properties have numerous potential applications such as sensors, rechargeable batteries, switchable membranes, optoelectronic devices, photo diodes and technological membranes<sup>1,2</sup>. Among the conducting polymers, polyaniline is unique due to its high conductivity, ease of synthesis, light weight, high stress, good environmental stability, low cost and along with low operational voltage making it a good candidate in the development of actuators<sup>3-5</sup>. Polyaniline can be synthesized by either oxidative chemical or electro chemical polymerization of monomer in liquid phase<sup>6</sup>. However, the major disadvantage of polyaniline is its insolubility in common organic solvents and its infusibility. One possible method for preparing soluble polyaniline is with the help of substituted groups<sup>7,8</sup>.

Polyaniline can be prepared as a composite with the incorporation of various inorganic particles like Nb<sub>2</sub>O<sub>5</sub><sup>9</sup>, ZrO<sub>2</sub><sup>10</sup>, Dy<sub>2</sub>O<sub>3</sub><sup>11</sup>, iron oxalate<sup>12</sup>, polyvinyl alcohol<sup>13</sup>, iron oxide<sup>14</sup> etc., However, to the best of our knowledge, no work has been reported on the preparation of polyaniline composites using P<sub>2</sub>O<sub>5</sub> by chemical oxidation method. Phosphorus pentaoxide, a strong dehydrating agent, removes a molecule of water from organic and inorganic compounds and thus acting as a powerful

desiccant. The aim of the present work is to synthesize polyaniline/P<sub>2</sub>O<sub>5</sub> composites with different mole percentages and characterize them using FTIR, UV-visible, XRD, SEM, EDAX, AFM and TGA.

### EXPERIMENTAL

Aniline, ammonium persulfate, P<sub>2</sub>O<sub>5</sub>, DMF (all from Merck, India), sulphuric acid (Rankem, India), acetone, methanol and distilled water were used throughout the experiment. All the chemicals used were of analytical grade.

**Synthesis of polyaniline:** A low temperature (0-6°) chemical oxidation method was used to synthesize polyaniline. Initially aniline (0.8 M) was dissolved in 150 mL of distilled water to which 1.25 M of H<sub>2</sub>SO<sub>4</sub> was added. Ammonium persulfate (0.8 M) used as an oxidant in the experiment was dissolved in 20 mL of distilled water separately. This solution was added slowly to the above reaction mixture with thorough and continuous stirring. The resultant dark green solution was filtered and washed sequentially with distilled water, acetone and methanol. The samples were then oven dried at 60 °C for 24 h. The synthesized polyaniline was finally ground to a fine powder and used for further studies.

**Synthesis of polyaniline/P<sub>2</sub>O<sub>5</sub> Composites:** The P<sub>2</sub>O<sub>5</sub> powder (99.99 % pure, Merck) was used for the preparation of the polyaniline/P<sub>2</sub>O<sub>5</sub> composites. To an already prepared

†International Conference on Nanoscience & Nanotechnology, (ICONN 2013), 18-20 March 2013, SRM University, Kattankulathur, Chennai, India

solution of aniline (0.8 M) containing 1.25 M sulphuric acid,  $P_2O_5$  in powder form was taken in the required quantity (8-12 g) and added slowly with continuous stirring. Ammonium persulfate (0.8 M) was then added drop wise to this reaction mixture in the form of an aqueous solution. The solution mixture was stirred for 0.5 h and allowed to stand for a further period of 3 h. The resultant product was filtered, washed with distilled water, acetone and methanol and dried in an oven at 60 °C for 24 h. The resultant material was ground to a fine powder and used for further studies.

**Characterization techniques:** The chemical structure of the polyaniline and polyaniline/ $P_2O_5$  powders were studied from the infrared spectra (Perkin Elmer FTIR spectrometer-Model RXI) in the range of 4000  $cm^{-1}$  to 400  $cm^{-1}$ . The KBr pellet technique was adopted to prepare the sample for recording the IR spectra. The UV-VIS spectra (Perkin Elmer - Model Lambda 35) of the samples, which were dispersed in DMF, were recorded from 190 nm-1100 nm.

X-ray diffraction analyses (Bruker AXS B8 advance) were carried out in the  $2\theta$  range from 10°-70° and the patterns were matched with the standard pattern provided in the JCPDS file. Morphological study and the elemental analysis of the samples of the polyaniline and polyaniline/ $P_2O_5$  were observed using a scanning electron microscope (Model JSM-6390LV) operating at 20 KV at a magnification of 5000 X. The topographical analyses were done using AFM (Park AFM (XE-100)) in the scan range of 10 × 10  $\mu m$ . Thermo gravimetric analysis (SDTQ 600 V8.0 Build 95) of polyaniline and polyaniline/ $P_2O_5$  was carried out at a heating rate of 10 °C/min up to 1000 °C in  $N_2$  atmosphere.

## RESULTS AND DISCUSSION

**FTIR analysis of composites:** FTIR spectra of polyaniline and polyaniline/ $P_2O_5$  composites (Fig. 1) show the assigning of the main characteristics peaks of polyaniline as follows: the band at 3760  $cm^{-1}$  is responsible for N-H stretching, the peak at 3433  $cm^{-1}$  accounts for the O-H stretching of water molecules physisorbed the polyaniline backbone, the bands at 1638  $cm^{-1}$

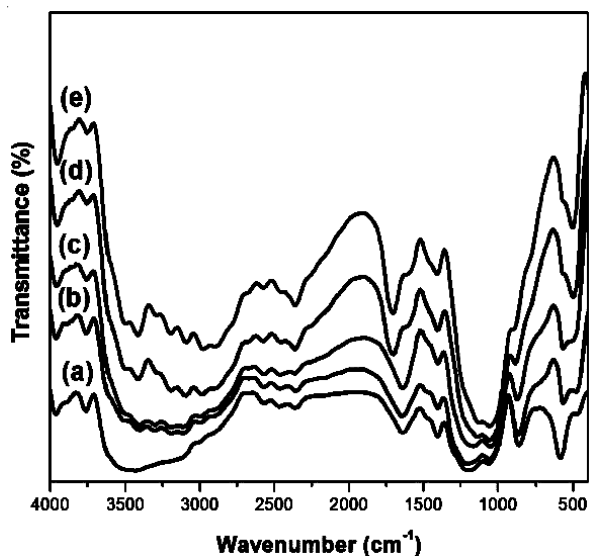


Fig. 1. FT-IR spectra of (a) Pure PANI (b)  $P_2O_5$  (c) PANI/8 $P_2O_5$  (d) PANI/10 $P_2O_5$  (e) PANI/12 $P_2O_5$

and 1404  $cm^{-1}$  are attributed to C=C and C=N stretching modes of vibration for quinonoid and benzenoid rings of polyaniline and the peak at 1197  $cm^{-1}$  is due to C-N stretching mode of benzenoid units (in-plane bending mode) and the quinonoid unit of polyaniline (N=Q=N). The assignment of peaks reveals that the synthesized product is polyaniline<sup>10, 15-17</sup>.

The band at 863  $cm^{-1}$  is an evidence for C-H out of plane bending vibration. The peaks at 1234  $cm^{-1}$  and 1022  $cm^{-1}$  belong to the P=O stretching of  $P_2O_5$ <sup>18</sup>. A peak between 1000-1090  $cm^{-1}$  confirms the inclusion of  $P_2O_5$  in polyaniline/ $P_2O_5$  composites.

**UV-visible spectra of composites:** UV-visible absorption spectra (Fig. 2) for polyaniline and polyaniline/ $P_2O_5$  composites show four absorption bands of polyaniline at 298, 355, 434 and 831 nm. The bands at 298, 355 and 434 nm are attributed to the  $\pi-\pi^*$  and polaron- $\pi^*$  transitions of the benzenoid ring and exciton absorption of quinoid rings respectively in polyaniline<sup>19,20</sup>. The polaron band around 831 nm characterizes protonation and it is identical to that of emeraldine salt form of polyaniline<sup>21</sup>.

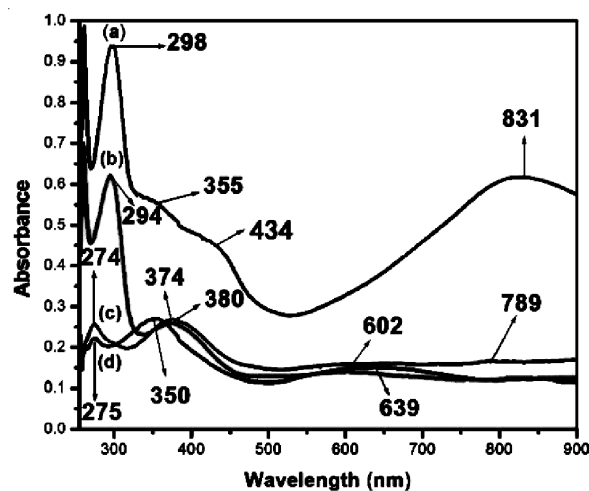


Fig. 2. UV-visible spectra of (a) PANI (b) PANI/8 $P_2O_5$  (c) PANI/10 $P_2O_5$  (d) PANI/12 $P_2O_5$

In addition, in the polyaniline/ $P_2O_5$  composites, a blue shift of the absorption band could be observed as the  $\pi-\pi^*$  transition in the benzenoid ring is shifted to 374, 380 and 350 nm. The exciton absorption band of quinoid rings also shifts to 565-663 nm in the polyaniline/ $P_2O_5$  composites due to the interaction of polyaniline with  $P_2O_5$ .

**XRD analysis:** Typical XRD patterns of polyaniline and polyaniline/ $P_2O_5$  composites are shown in Fig. 3. The patterns of polyaniline exhibiting two peaks ( $2\theta$ ) at 19° and 21° can be ascribed to the presence of periodicity parallel and perpendicular to the polymer chain respectively<sup>22-24</sup>. In polyaniline/ $P_2O_5$  composites, the peak at 25° exhibits a broader peak than polyaniline due to the interaction of  $P_2O_5$  with polyaniline, thereby indicating the possibility that the crystalline behaviour of polyaniline gets affected slightly by the increasing content of  $P_2O_5$ . The average particle size (D), calculated using the scherrer formula ( $D = K\lambda/\beta \cos\theta$ ) are shown in Table-1, wherein it is clearly seen that the average particle size decreases with the increasing content of  $P_2O_5$ .

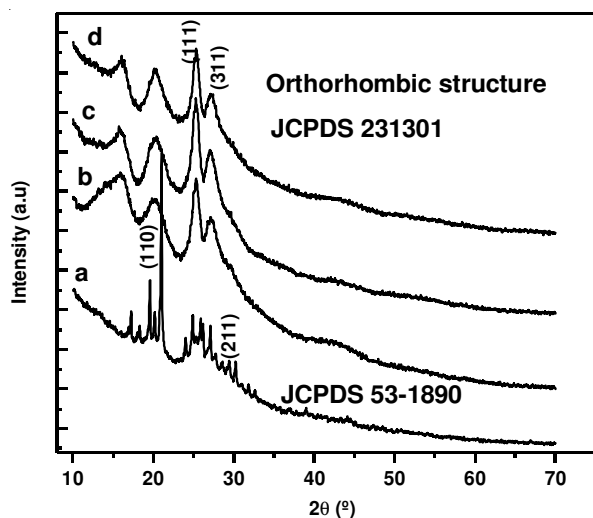


Fig. 3. XRD spectra of (a) PANI (b) PANI/8P<sub>2</sub>O<sub>5</sub> (c) PANI/10P<sub>2</sub>O<sub>5</sub> (d) PANI/12P<sub>2</sub>O<sub>5</sub>

Polymer/ Polymer composite	Position 2θ (°)	FWHM (°)	d-spacing (Å)		Particle Size D (in nm)
			Calculated	JCPDS	
PANI	29.4451	0.2244	3.367	3.03357	38
PANI/ 8P <sub>2</sub> O <sub>5</sub>	25.3611	0.6731	3.508	3.5113	12.63
PANI/ 10P <sub>2</sub> O <sub>5</sub>	25.3346	0.6731	3.897	3.5156	12.58
PANI/ 12P <sub>2</sub> O <sub>5</sub>	25.3414	0.7478	3.895	3.51466	11.32

**SEM and EDAX analysis:** The morphologies of polyaniline, P<sub>2</sub>O<sub>5</sub> and polyaniline/P<sub>2</sub>O<sub>5</sub> composites were compared at different magnifications (500 and 5000 X). From the Fig. (4a) a granular texture could be observed for polyaniline containing clusters of globules<sup>9,15,25</sup>. The spherical nature of P<sub>2</sub>O<sub>5</sub> particles can be seen from Fig. 4b. With increasing amounts of P<sub>2</sub>O<sub>5</sub> (8 g, 10 g, 12 g) there is a visible increase in the grain size suggesting to intermixing of P<sub>2</sub>O<sub>5</sub> particles with polyaniline (Fig. 4c-e). polyaniline/P<sub>2</sub>O<sub>5</sub> composites show a transformation from granular (polyaniline) to spherical morphology. The SEM images also help us to draw the conclusion that the doping of P<sub>2</sub>O<sub>5</sub> strong affects the morphology of

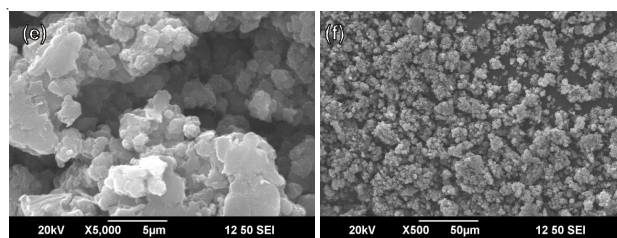
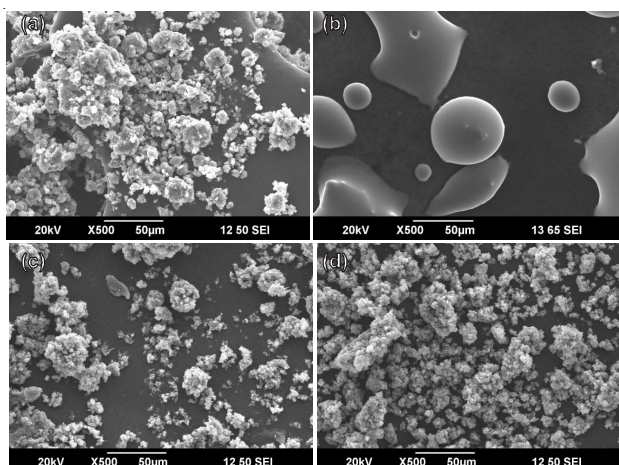


Fig. 4. SEM Micrographs a) PANI, b) P<sub>2</sub>O<sub>5</sub>, c) PANI/8P<sub>2</sub>O<sub>5</sub>, d) PANI/10P<sub>2</sub>O<sub>5</sub>, e) PANI/12P<sub>2</sub>O<sub>5</sub>

polyaniline. The EDAX analysis of the composite sample (Fig. 5) shows the presence of the constituents of both P<sub>2</sub>O<sub>5</sub> and polyaniline.

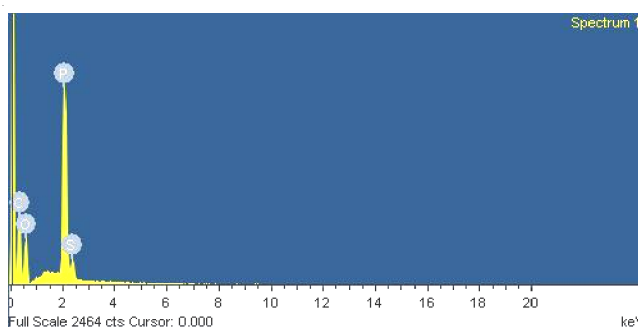


Fig. 5. EDAX spectrum of PANI/12P<sub>2</sub>O<sub>5</sub>

**Atomic force microscopy analysis:** Fig. 6a-6d show the three dimensional (3D) AFM images of polyaniline and polyaniline/P<sub>2</sub>O<sub>5</sub> composites taken in a scan range of 10 × 10 µm. The topographical view of polyaniline shows deep valleys in between polymer chains. Well defined grains of approximately 200 nm sizes and with irregular tips projected to the surface are observed in the 3D images of polyaniline<sup>26,27</sup>. The deep valleys in the polymer chain disappear due to the increasing amount of P<sub>2</sub>O<sub>5</sub> particles being accommodated in the polymer chain. The uniform grain sizes of approximately 100 nm are projected on the surface as seen in the 3D images of polyaniline/P<sub>2</sub>O<sub>5</sub> composites.

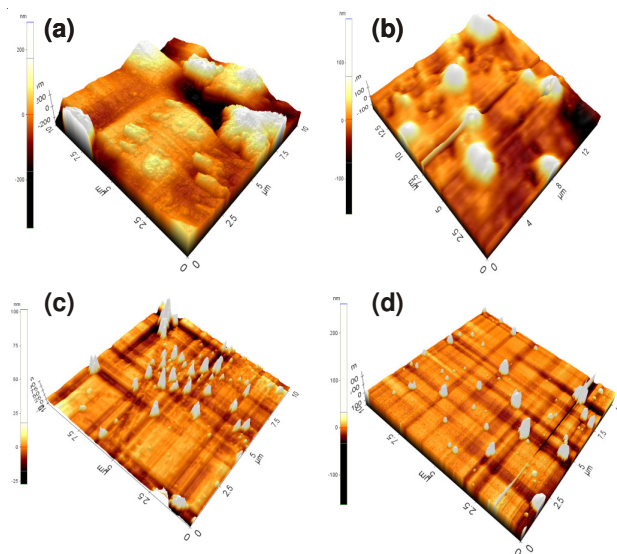


Fig. 6. AFM images of a) 3D PANI, b) 3D PANI/8P<sub>2</sub>O<sub>5</sub>, c) 3D PANI/10P<sub>2</sub>O<sub>5</sub>, d) 3D PANI/12P<sub>2</sub>O<sub>5</sub>

TABLE-2  
THERMOGRAM RESULTS FOR PANI AND PANI/ P<sub>2</sub>O<sub>5</sub> COMPOSITES

Polymer/polymer composite	Range (°C)			Final decomposition (in °C)	Residue (in %)	Final total wt. loss (in %)
	1 <sup>st</sup> wt. loss (due to loss of moisture)	2 <sup>nd</sup> wt. loss (due to loss of dopant ion)	3 <sup>rd</sup> wt. loss (due to P <sub>2</sub> O <sub>5</sub> addition)			
PANI	50-69	172-211	--	> 342	15.7	84.3
PANI/8P <sub>2</sub> O <sub>5</sub>	45-165	240-287	366-380	> 754	32.0	68.0
PANI/10P <sub>2</sub> O <sub>5</sub>	49-79	185-210	370-381	> 801	32.7	67.3
PANI/12P <sub>2</sub> O <sub>5</sub>	43-76	200-276	376-390	> 810	20.9	79.0

**Thermogravimetric analysis:** Thermogravimetric analyses of polyaniline and polyaniline/P<sub>2</sub>O<sub>5</sub> composites were done in the temperature range of 0-1000 °C and are shown in Fig. 7a-7d. The thermogram of polyaniline exhibits a three-step weight loss process. In the first step, a weight loss in the

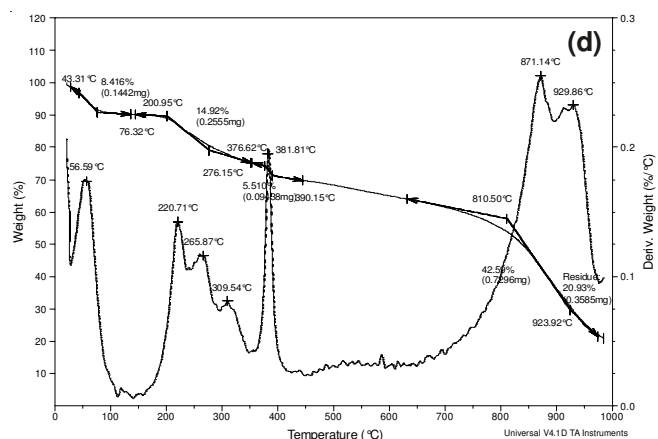
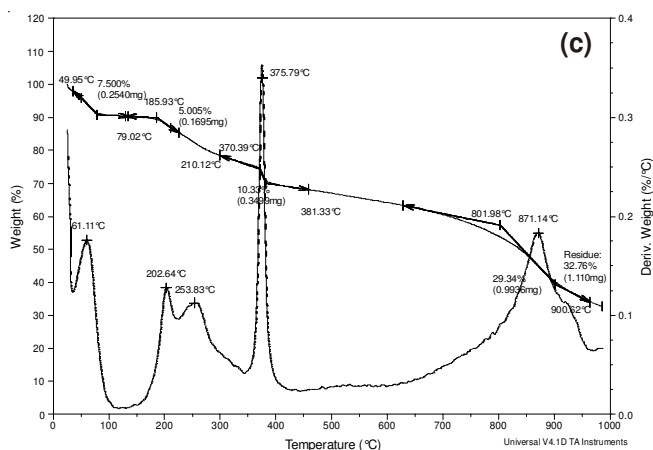
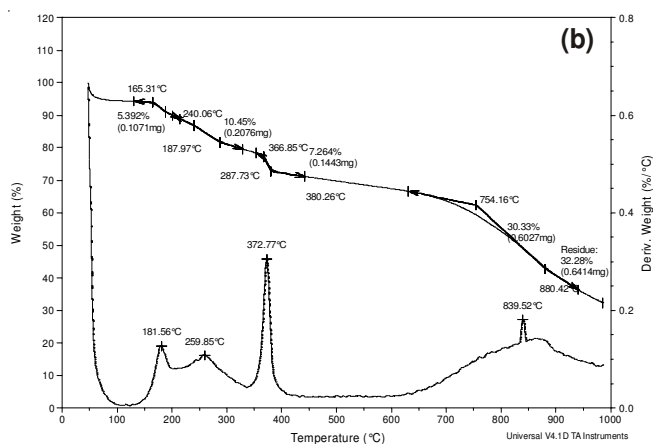
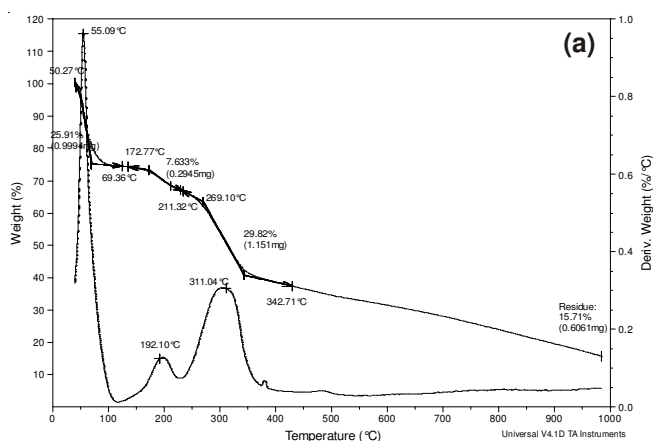


Fig. 7. TGA spectrum a) PANI b) PANI/8P<sub>2</sub>O<sub>5</sub> c) PANI/10 P<sub>2</sub>O<sub>5</sub> d) PANI/12 P<sub>2</sub>O<sub>5</sub>

range of 50-69 °C is attributed to the expulsion of water molecules from the polymer chain. The second weight loss occurring between 172-211 °C is associated with the loss of dopant ion from the polymer matrix. The third weight loss beyond 342 °C is due to the complete degradation and decomposition of the polymer after elimination of the dopant ion<sup>16,28,29</sup>.

The TGA curves of polyaniline/P<sub>2</sub>O<sub>5</sub> composites have a four step weight loss, with the first three steps similar to that of pure polyaniline (Table-2). The additional fourth step weight loss in polyaniline/P<sub>2</sub>O<sub>5</sub> composites around 366-390 °C may be due to the decomposition of P<sub>2</sub>O<sub>5</sub> in the composites. From Table-2, it is clear that, as the quantity of P<sub>2</sub>O<sub>5</sub> is increased, the bonding becomes stronger and hence a reduction in the final weight loss is observed in the polymer composites and hence it could be implied that the samples become more stable with respect to temperature.

## Conclusion

The polyaniline/P<sub>2</sub>O<sub>5</sub> composites are synthesized by a low temperature chemical oxidation method. Structural changes, transitions, crystallinity, morphology, grain size and stability of polyaniline/P<sub>2</sub>O<sub>5</sub> composites are found to be affected by the concentration of P<sub>2</sub>O<sub>5</sub>. A strong interaction between polyaniline and P<sub>2</sub>O<sub>5</sub> could be inferred from the FT-IR and UV-visible spectroscopic results. The XRD analysis reveals that crystallinity of polyaniline is affected mildly with increasing P<sub>2</sub>O<sub>5</sub> content. The changes in the morphology of polyaniline due to the addition of P<sub>2</sub>O<sub>5</sub> could be observed from the SEM images. The EDAX spectrum clearly shows and confirms the presence of elemental polyaniline and P<sub>2</sub>O<sub>5</sub>. AFM analysis shows the topographical view of polyaniline with deep valleys between the polymer chains, while in polyaniline/P<sub>2</sub>O<sub>5</sub> composites the deep valleys between the polymer chains are

found to disappear with increasing concentrations of P<sub>2</sub>O<sub>5</sub>. The thermal stability of the composite materials shows reduced decomposition compared to pure polyaniline.

### REFERENCES

1. J.-C. Xu, W.-M. Liu and H.-L. Li, *Mater. Sci. Eng. C*, **25**, 444 (2005).
2. P.R. Somani, R. Marimuthu and A.B. Mandale, *Polym. J.*, **42**, 2991 (2010).
3. R. Cruz-Silva, A. Escamilla, M.E. Nicho, G. Padron, A. Ledezma-Perez, E. Arias-Marin, I. Moggio and J. Romero-Garcia, *Eur. Polym. J.*, **43**, 3471 (2007).
4. Z.F. Du, C.C. Li, L.M. Li, M. Zhang, S.J. Xu and T.H. Wang, *Mater. Sci. Eng. C*, **29**, 1794 (2009).
5. C.-H. Ho, C.-D. Liu, C.-H. Hsieh, K.-H. Hsieh and S.-N. Lee, *Synth. Met.*, **158**, 630 (2008).
6. J.Y. Kim, S.J. Kwon and D.W. Ihm, *Curr. Appl. Phys.*, **7**, 205 (2007).
7. A.T. Ramaprasad, V. Rao, G. Sanjeev, S.P. Ramanani and S. Sabharwal, *Synth. Met.*, **159**, 1983 (2009).
8. A.G. Yavuz, A. Uygun and V.R. Bhethanabotla, *Carbohydr. Polym.*, **75**, 448 (2009).
9. Y.T. Ravikiran, M.T. Lagare, M. Sairam, N.N. Mallikarjuna, B. Sreedhar, S. Manohar, A.G. MacDiarmid and T.M. Aminabhavi, *Synth. Met.*, **156**, 1139 (2006).
10. S.X. Wang, Z.C. Tan, Y.S. Li, L.X. Sun and T. Zhang, *Thermochim. Acta*, **441**, 191 (2006).
11. K. Sangshetty, A.R. Koppalkar, M. Revansiddappa and S. Ekilekar, *Physica B*, **404**, 1883 (2008).
12. C. Visy, G. Bencsik, Z. Nemeth and A. Vertes, *Electrochim. Acta.*, **53**, 3942 (2008).
13. A. Mirmohseni and G.G. Wallace, *Polym. J.*, **44**, 3523 (2003).
14. J.C. Apesteguy and S.E. Jacobo, *Physica B*, **354**, 224 (2004).
15. K. Gupta, P.C. Jana and A.K. Meikap, *Synth. Met.*, **160**, 1566 (2010).
16. A.Y. Arasi, J. Juliet, L. Jeyakumari, B. Sundaresan, V. Dhanalakshmi and R. Anbarasan, *Spectrochim. Acta A*, **74**, 1229 (2009).
17. M. Irimia-Vladu and J.W. Fergus, *Synth. Met.*, **156**, 1401 (2006).
18. I. Ardelean and C. Horea, *Optoelectron. Adv. M.*, **8**, 1111 (2006).
19. S.G. Pawar, S.L. Patil, M.A. Chougule, S.N. Achary and V.B. Patil, *Int. J. Polymer. Mater.*, **60**, 244 (2011).
20. H.L. Tai, Y.D. Jiang, G.Z. Xie and J.S. Yu, *J. Mater. Sci. Technol.*, **26**, 605 (2010).
21. A.G. Yavuz and A. Gok, *Synth. Met.*, **157**, 235 (2007).
22. N. Binitha, V. Suraja, Z. Yaakob and S. Sugunan, *Sains Malays.*, **40**, 215 (2011).
23. S. Srivastava, S. Kumar and Y.K. Vijay, *Int. J. Hydrogen Energy*, **37**, 3825 (2011).
24. V. Singh, S. Mohan, G. Singh, P.C. Pandey and R. Prakash, *Sens. Actuators B*, **132**, 99 (2008).
25. S. Srivastava, S. Kumar, V.N. Singh, M. Singh and Y.K. Vijay, *Int. J. Hydrogen Energy*, **36**, 6343 (2011).
26. G. Milczarek, *React. Funct. Polym.*, **68**, 1542 (2008).
27. H.-J. Kim, S.H. Park and H.-J. Park, *Radiat. Phys. Chem.*, **79**, 894 (2010).
28. S. Bhadra and D. Khastgir, *Synth. Met.*, **159**, 1141 (2009).
29. A.H. Elsayed, M.S. Mohy Eldin, A.M. Elsyed, A.H. Abo Elazm, E.M. Younes and H.A. Motaweh, *Int. J. Electrochem. Sci.*, **6**, 206 (2011).